

Calculations of Shear, Bulk viscosities and Electrical conductivity in Polyakov-Quark-Meson model

Pracheta Singha¹, Aman Abhishek², Guru Kadam³, Sabyasachi Ghosh⁴, Hiranmaya Mishra²

¹*Center for Astroparticle Physics and Space, Bose Institute, Block-EN,
Sector-V, Salt Lake, Bidhan Nagar, Kolkata - 700091, India*

²*Theory Division, Physical Research Laboratory, Navrangpura, Ahmedabad 380 009, India*

³*Department of theoretical Physics, Tata Institute of fundamental Research, Homi Bhabha Road, Mumbai 400005, India and*

⁴*Department of Physics, University of Calcutta, 92, A. P. C. Road, Kolkata - 700009, India*

We have evaluated the transport coefficients of quark and hadronic matter in the frame work of Polyakov-Quark-Meson model. The thermal widths of quarks and mesons, which inversely control the strength of these transport coefficients, are obtained from the imaginary part of their respective self-energies at finite temperature. Due to the threshold conditions of their self energies, some limited temperature regions of quark and hadronic phase become relevant for our numerical predictions on transport coefficients, which are grossly in agreement with earlier results.

I. INTRODUCTION

Microscopic calculations of transport coefficients like the shear and bulk viscosities of quark and hadronic matter are one of the contemporary research interest in the field of heavy ion physics. These coefficients are relevant not only because they enter as inputs for dissipative hydrodynamical simulations, but also through their dependence on system parameters like temperature and chemical potential, they can indicate the location of phase transition in the phase diagram [1]. Indeed, the smallness of the shear viscosity to entropy density ratio η/s to explain the data of elliptic flow [2, 3] and its connection with the Kovtun-Son-Starinets (KSS) lower bound, $\eta/s = 1/4\pi$, has spurred many activities to investigate this coefficient theoretically [1, 4–33]. Among them, Refs. [4–6] and Refs. [7–16] have calculated η of quark matter and hadronic matter respectively, whereas Refs. [17–25] have calculated η for both of the mediums by covering the entire range of temperature (T). Some simulation based calculations for η are addressed in Refs. [26–29]. These investigations provide a grossly settled picture of the temperature dependence of viscosity to entropy density ratio (η/s) which exposes a minimum near transition temperature T_c , similar to helium, nitrogen, and water [1]. However the numerical results of these calculations near critical temperature seem to differ by order of magnitude. For example Refs. [7, 10], Refs. [9, 11, 32] and Refs. [8] have predicted $\eta \approx 0.001 \text{ GeV}^3$, $\eta \approx 0.002 - 0.003 \text{ GeV}^3$ and $\eta \approx 0.4 \text{ GeV}^3$ respectively.

Similar to the shear viscosity, bulk viscosity (ζ) has a long list of references as well [9, 14–22, 32–50], where most of the calculations are done in the vanishing baryonic chemical potential. Hard thermal loop (HTL) calculations of ζ have been done by Ref. [35]. The calculations of effective models of quantum chromo dynamics (QCD) like Nambu-Jona-Lasinio (NJL) model [18–21, 41, 50] and linear sigma model (LSM) [17, 34, 39] have explored the temperature dependence of ζ for both quark and hadronic phases. Refs. [9, 14–16, 45, 46, 48] are the effective hadronic-model calculations valid for the hadronic

phase only. Some calculations in quark temperature domain [37, 42, 43] and some in hadronic domain [14, 16] have observed an increasing nature of $\zeta/s(T)$ near T_c , which might be associated with the peak, obtained at transition point in the full temperature range plot of $\zeta/s(T)$ [17, 39, 50]. Although, instead of this peak structure, Refs. [15, 21, 47] have predicted decreasing nature of $\zeta/s(T)$. The order of magnitude of ζ and ζ/s from different model calculations varies widely covering a range of values from 10^{-5} GeV^3 [46] to 10^{-2} GeV^3 [18] and 10^{-3} [46] to 10^0 [18] respectively. Thus we see that there are uncertainties in nature as well as in numerical values of $\zeta(T)$ and $\zeta/s(T)$, which require further investigations.

Another transport coefficient, we are interested in, is the electrical conductivity σ , which has been studied by a large number of Lattice QCD calculations [51–57], predicting a wide band in their numerical results. Besides these first principle based calculations, some simulation based calculations using transport codes [58–60] and other model dependent calculations [19, 61–68] for σ have also been done. Most of the earlier works [19, 58–62, 64, 65, 68] have observed the decreasing nature of $\sigma(T)/T$ in hadronic temperature domain [19, 58, 64, 65, 68] and increasing trends in the quark temperature domain [19, 57–62]. However, Refs. [62, 63, 66] have seen that σ/T increases with T in hadronic phase. Not only the thermal behaviour of this dimensionless ratio (σ/T), the uncertainty also appears in their numerical values, whose approximate range may be considered as $\sigma/T \approx 10^{-3}$ to 10^{-2} for hadronic phase and $\sigma/T \approx 10^{-3}$ to 10^{-1} for quark phase.

Above discussions thus essentially point to the unsettled issues on transport coefficients of quark and hadronic matter, which motivates us for the current investigation. In present article, we have calculated different transport coefficients in Polyakov-Quark-Meson (PQM) model, which has not been investigated so far, to the best of our knowledge. Here, we have evaluated one-loop self-energy diagrams of quark and meson to obtain their relaxation times or thermal widths, where we have analyzed the detailed branch cut structures of their self-

energies. Using these, we have estimated different transport coefficients in some specific temperature regions of quark and hadronic phase and then, they are compared with the earlier estimations using different models.

The paper is organized as follows. Next section addresses the formalism part of the PQM model and transport coefficients. The analytic structure of the self-energies and their contributions to the transport coefficients of quark and hadronic matter are rigorously discussed in the result section, followed by a summary and conclusions in the last section.

II. FORMALISM

A. Thermodynamics of two-flavor PQM model and meson masses

To incorporate aspects of chiral symmetry breaking and its restoration in a medium as well as confinement-deconfinement transition, we shall adopt here the Polyakov loop extended quark meson model. This is an extension of linear sigma model that provides an effective realization of chiral symmetry. Coupling the quarks and meson degrees of freedom to the expectation values of the Polyakov loop, the physics of confinement is expected to be taken into account here. We confine the investigation here regarding the transport coefficients to the two flavor version of the PQM model. The corresponding Lagrangian density is given as

$$\begin{aligned} \mathcal{L} = & \bar{\psi} (i\gamma^\mu D_\mu - m_q - g(\sigma + i\gamma_5 \vec{\tau} \cdot \pi)) \psi \\ & + \frac{1}{2} [\partial_\mu \sigma \partial^\mu \sigma + \partial_\mu \vec{\pi} \partial^\mu \vec{\pi}] \\ & - U_\chi(\sigma, \vec{\pi}) - U_P(\Phi, \bar{\Phi}) . \end{aligned} \quad (1)$$

Here $\psi = (u, d)$ is a $SU(2)_f$ isodoublet interacting with the isovector $(\sigma, \vec{\pi})$ field. The quark field is also coupled to a spatially constant temporal gauge field A_0 through the covariant derivative $D_\mu = \partial_\mu - ieA_\mu$; $A_\mu = \delta_{\mu 0}A_0$. The mesonic potential $U_\chi(\sigma, \vec{\pi})$ essentially describes the chiral symmetry breaking and is given by

$$U_\chi(\sigma, \vec{\pi}) = \frac{\lambda}{4}(\sigma^2 + \vec{\pi}^2 - v^2)^2 - C\sigma . \quad (2)$$

The parameters of the mesonic potential are chosen so that the chiral symmetry is spontaneously broken in the vacuum and the expectation values of the meson fields are $\langle \sigma \rangle = f_\pi$, $\langle \vec{\pi} \rangle = 0$, where $f_\pi = 93$ MeV is the pion decay constant. The constant C is fixed from partial conserved axial current leading to $c = f_\pi m_\pi^2$, with $m_\pi = 138$ MeV being the pion mass. $v^2 = f_\pi^2 - m_\pi^2/\lambda$ is obtained by minimizing the potential. The coupling λ is fixed from the sigma mass $m_\sigma^2 = m_\pi^2 + 2\lambda f_\pi^2$. With $m_\sigma = 600$ MeV leads to $\lambda = \frac{(m_\sigma^2 - m_\pi^2)}{2f_\pi^2} \simeq 19.7$. The Yukawa coupling g is fixed from the requirement that the constituent quark mass in vacuum $m_q = gf_\pi$. With $m_q = 300$ MeV leads to $g \simeq 3.3$.

The Polyakov loop potential $U_P(\Phi, \bar{\Phi})$ in the Lagrangian in Eq.(1) includes the physics of color confinement. The Polyakov loop variable $\Phi = \Phi(\vec{x}) = \frac{1}{N_c} \langle \text{tr}_c \mathcal{P}(\vec{x}) \rangle_\beta$, where $\mathcal{P} = \mathcal{P} \exp \left(i \int_0^\beta dx_0 A_0(x_0, \vec{x}) \right)$, is an order parameter for confinement-deconfinement transition in the infinitely heavy quark limit. It vanishes in the confined phase and attains non-zero value in deconfined phase. The explicit form of the potential $U_P(\Phi, \bar{\Phi})$ is not known from first principle calculations and the following is a fit taken from lattice results [69]

$$U_P(\Phi, \bar{\Phi}) = T^4 \left[-\frac{b_2(T)}{2} \bar{\Phi} \Phi - \frac{b_3}{2} (\Phi^3 + \bar{\Phi}^3) + \frac{b_4}{4} (\bar{\Phi} \Phi)^2 \right] \quad (3)$$

with the coefficients given as $b_2(T) = 6.75 - 1.95(\frac{T_0}{T}) + 2.625(\frac{T_0}{T})^2 - 7.44(\frac{T_0}{T})^3$, $b_3 = 0.75$, $b_4 = 7.5$. The parameter T_0 corresponds to the transition temperature of Yang-Mills theory. However, for the full dynamical QCD, there is a flavor dependence on $T_0(N_f)$. For two flavors we take it to be $T_0(N_f = 2) = 192$ MeV as in Ref.[69].

To calculate the bulk thermodynamical properties of the system we use a mean field approximation for the meson and the Polyakov fields while retaining the quantum and thermal fluctuations of the quark fields. The thermodynamic potential can then be written as

$$\Omega(T, \mu) = \Omega_{\bar{q}q} + U_\chi + U_P(\Phi, \bar{\Phi}) . \quad (4)$$

The fermionic part of the thermodynamic potential is given as

$$\begin{aligned} \Omega_{\bar{q}q} = & -2N_f T \int \frac{d^3 p}{(2\pi)^3} \left[\ln \{1 + 3(\Phi + \bar{\Phi} e^{-\beta\omega_-}) e^{-\beta\omega_-} \right. \\ & \left. + e^{-3\beta\omega_-}\} + \ln \{1 + 3(\Phi + \bar{\Phi} e^{-\beta\omega_+}) e^{-\beta\omega_+} \right. \\ & \left. + e^{-3\beta\omega_+}\} \right] \end{aligned} \quad (5)$$

modulo a divergent vacuum part. In the above $\omega_\mp = E_p \mp \mu$, with the single particle quark/anti-quark energy $E_p = \sqrt{\vec{p}^2 + m_q^2}$. The mean fields are obtained by minimizing Ω with respect to σ , Φ and $\bar{\Phi}$. That is $\frac{\partial \Omega}{\partial \sigma} = \frac{\partial \Omega}{\partial \Phi} = \frac{\partial \Omega}{\partial \bar{\Phi}} = 0$

The σ and π masses are given by the curvature of Ω at the global minimum by $M_\sigma^2 = \frac{\partial^2 \Omega}{\partial \sigma^2}$ and $M_{\pi_i}^2 = \frac{\partial^2 \Omega}{\partial \pi_i^2}$. These equations lead to the masses of the σ and π given as

$$M_\sigma^2 = m_\pi^2 + \lambda(3\sigma^2 - f_\pi^2) + g^2 \frac{\partial \rho_s}{\partial \sigma} , \quad (6)$$

with

$$\rho_s = 6N_f g \sigma \int \frac{d^3 p}{(2\pi)^3} \frac{1}{E_p} [f_- + f_+] \quad (7)$$

and

$$M_\pi^2 = m_\pi^2 + \lambda(\sigma^2 - f_\pi^2) + g^2 \frac{\partial \rho_{ps}}{\partial \pi} , \quad (8)$$

with

$$\vec{p}_{ps} = \langle \bar{q}i\gamma_5 \vec{\tau}q \rangle = 6N_f g \vec{\pi} \int \frac{d^3 p}{(2\pi)^3} \frac{1}{E_P} [f_- + f_+]. \quad (9)$$

In the above, f_{\mp} are the distribution functions for the quarks and anti quarks, given as

$$\begin{aligned} f_- &= \frac{\Phi e^{-\beta\omega_-} + 2\bar{\Phi}e^{-2\beta\omega_-} + e^{-3\beta\omega_-}}{1 + 3\Phi e^{-\beta\omega_-} + 3\bar{\Phi}e^{-2\beta\omega_-} + e^{-3\beta\omega_-}}, \\ &\text{and} \\ f_+ &= \frac{\bar{\Phi}e^{-\beta\omega_+} + 2\Phi e^{-2\beta\omega_+} + e^{-3\beta\omega_+}}{1 + 3\bar{\Phi}e^{-\beta\omega_+} + 3\Phi e^{-2\beta\omega_+} + e^{-3\beta\omega_+}}. \end{aligned} \quad (10)$$

We have set the expectation value of pion field to be zero, i.e. $\vec{\pi} = 0$ so that the constituent quark mass becomes $m_q^2 = g^2(\sigma^2 + \vec{\pi}^2) = g^2\sigma^2 = g^2f_\pi^2$.

B. Transport coefficients

Our aim is to calculate different transport coefficients like shear viscosity η , bulk viscosity ζ and electrical conductivity σ using the dynamics of PQM model. Since the medium constituents for 2 flavor PQM model are u , d quarks and π , σ mesons, so we will address here the expressions of different transport coefficients for quark and mesonic components one by one. Let us first come to the expression of shear viscosity for quark component, which one can derive either from relaxation time approximation (RTA) in Kinetic theory approach [17, 31, 33] or from quasi-particle one-loop anatomy in Kubo approach [9, 20, 70]. Only Fermi-Dirac (FD) distribution function of quark will be replaced by f_{\pm} of Eq. (10) because of the Polyakov loop extension in this effective QCD model. For $\mu_q = 0$, $f_+ = f_- = f_Q$ (say) in Eq. (10) and in terms of f_Q , shear viscosity of quark component will be

$$\eta_Q = \frac{2g_Q\beta}{15} \int \frac{d^3 \vec{k}}{(2\pi)^3 \Gamma_Q} \left(\frac{\vec{k}^2}{\omega_Q^k} \right)^2 f_Q \{1 - f_Q\}, \quad (11)$$

where Γ_Q is the thermal width of quark and $g_Q = 2 \times 2 \times 3 = 12$ is total degeneracy factor for quarks due to spin, flavor and color charges.

Similarly, shear viscosity of pion and sigma meson components can also be derived from RTA [17, 31, 33] or Kubo [9, 10, 70] approach and they can be written in a generalized form [9, 10, 17, 31, 33, 70]:

$$\eta_M = \frac{g_M\beta}{15} \int \frac{d^3 \vec{k}}{(2\pi)^3 \Gamma_M} \left(\frac{\vec{k}^2}{\omega_M^k} \right)^2 n_M(\omega_M^k) \{1 + n_M(\omega_M^k)\}, \quad (12)$$

where $n_M^k(\omega_M^k) = 1/\{e^{\beta\omega_M^k} - 1\}$ is Bose-Einstein (BE) distribution and Γ_M is thermal width of corresponding mesons $M = \pi, \sigma$. The isospin degeneracy factor $g_M = 3$ and 1 for $M = \pi$ and σ respectively.

Next, let us come to the standard expression of bulk viscosity ζ for quark and mesonic components [9, 17, 20, 33],

$$\begin{aligned} \zeta_Q &= 2g_Q\beta \int \frac{d^3 \vec{k}}{(2\pi)^3 \Gamma_Q} \left(\frac{(\frac{1}{3} - c_s^2)\vec{k}^2 - c_s^2 \frac{d}{d\beta^2}(\beta^2 m_Q^2)}{\omega_Q^k} \right)^2 \\ &\quad \times [f_Q \{1 - f_Q\}] \end{aligned} \quad (13)$$

and

$$\begin{aligned} \zeta_M &= g_M\beta \int \frac{d^3 \vec{k}}{(2\pi)^3 \Gamma_M} \left(\frac{(\frac{1}{3} - c_s^2)\vec{k}^2 - c_s^2 \frac{d}{d\beta^2}(\beta^2 m_M^2)}{\omega_M^k} \right)^2 \\ &\quad \times [n_M(\omega_M^k) \{1 + n_M(\omega_M^k)\}] \end{aligned} \quad (14)$$

respectively, where c_s is the speed of sound in the medium, which can be obtained from the thermodynamical quantities like pressure, energy density, entropy density.

Shear and bulk viscosities provide the estimation of some specified dissipative part of energy-momentum tensors in the form of their respective correlators. Similarly, electromagnetic current-current correlators of the medium is estimated from the electrical conductivity. Its standard expression for quark component is [20, 64]

$$\sigma_Q = \frac{2g_Q^e\beta}{3} \int \frac{d^3 \vec{k}}{(2\pi)^3 \Gamma_Q} \left(\frac{\vec{k}}{\omega_Q} \right)^2 f_Q \{1 - f_Q\}, \quad (15)$$

where degeneracy factor for 2 flavor quarks, associated with electrical conductivity is $g_Q^e = 2 \times 3 \times \left\{ \left(+\frac{2}{3} \right)^2 + \left(-\frac{1}{3} \right)^2 \right\} e^2 = \frac{10e^2}{3}$, with $e^2 = 4\pi/137$ in natural unit. Since σ meson is charge neutral so we can get electrical conductivity for pion component only and it is given by [64]

$$\sigma_\pi = \frac{g_\pi^e}{3T} \int \frac{d^3 \vec{k}}{(2\pi)^3 \Gamma_\pi} \left(\frac{\vec{k}}{\omega_\pi^k} \right)^2 [n_\pi(\omega_\pi^k) \{1 + n_\pi(\omega_\pi^k)\}], \quad (16)$$

where $g_\pi^e = 2e^2$ is isospin factor for charged pion - π^+ and π^- . So total values of all transport coefficients will be just addition of individual components *i.e.*

$$\eta_T = \eta_Q + \sum_{M=\pi,\sigma} \eta_M, \quad (17)$$

$$\zeta_T = \zeta_Q + \sum_{M=\pi,\sigma} \zeta_M, \quad (18)$$

$$\sigma_T = \sigma_Q + \sigma_\pi. \quad (19)$$

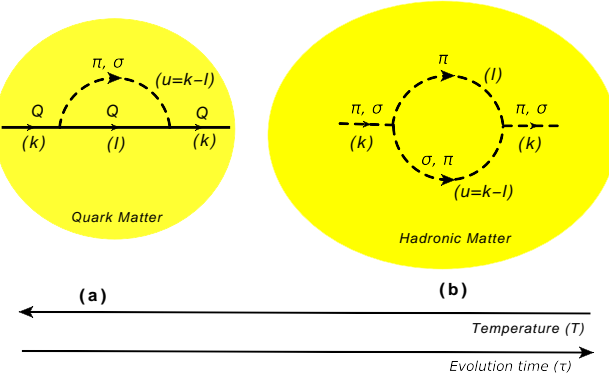


FIG. 1: Diagram (a) represents quark self-energy diagrams with quark-meson loop, where $M = \pi, \sigma$. Diagram (b) denotes π and σ meson self-energy diagram for $\pi\sigma$ and $\pi\pi$ loop respectively. The temperature and time evolution axis of fireball (yellow background) are to relate the diagrams with the phenomenological picture of heavy ion physics.

C. Thermal widths of quarks and mesons

To calculate thermal width of quarks and mesons, we have to extract relevant interaction part from the total Lagrangian density, addressed in Eq. (1). From Eq. (2), we can identify $\sigma\pi\pi$ interaction Lagrangian density:

$$\mathcal{L}_{\sigma\pi\pi} = \lambda f_\pi \sigma \vec{\pi}^2, \quad (20)$$

which will help us to calculate mesonic thermal widths Γ_M . Similarly to calculate quark thermal widths Γ_Q , we need to identify the QQM interaction part from Eq. (1). Expanding this QQM interaction Lagrangian density and dividing it into $QQ\pi$ and $QQ\sigma$ components, we get

$$\mathcal{L}_{QQ\pi} = ig \left[\sum_{Q=u,d} \bar{\psi}_Q \gamma^5 \pi^0 \psi_Q + \sqrt{2} \{ \bar{\psi}_u \gamma^5 \pi^+ \psi_d + \text{h.c.} \} \right] \quad (21)$$

and

$$\mathcal{L}_{QQ\sigma} = g \sum_{Q=u,d} \bar{\psi}_Q \sigma \psi_Q \quad (22)$$

respectively.

The quark thermal width, Γ_Q , can be estimated from the retarded part of the quark self-energy $\Sigma_{Q(QM)}^R$ at finite temperature for quark-meson (QM) loops, where $M = \pi, \sigma$ as shown in Fig 1(a). With the help of interaction Lagrangian densities (21) and (22), we obtain

$$\begin{aligned} \Gamma_Q(\vec{k}) &= -\frac{1}{m_Q} \sum_{M=\pi,\sigma} \left[\text{Tr} \left\{ (\not{k} + m_Q) \text{Im} \Sigma_{Q(QM)}^R(k) \right\} \right]_{k_0=\omega_Q^k} \\ &= \left[\int \frac{d^3 \vec{l}}{(2\pi)^3} \{ n_Q(\omega_Q^l) + n_\pi(\omega_\pi^u) \} \delta(k_0 + \omega_Q^l - \omega_\pi^u) \right. \end{aligned}$$

$$\begin{aligned} &\left. \frac{3g^2 \text{Tr} [(\not{k} + m_Q) \gamma^5 (\not{l} + m_Q) \gamma^5]}{m_Q (4\omega_Q^l \omega_\pi^u)} \right]_{l_0=-\omega_Q^l, k_0=\omega_Q^k} \\ &+ \left[\int \frac{d^3 \vec{l}}{(2\pi)^3} \{ n_Q(\omega_Q^l) + n_\sigma(\omega_\sigma^u) \} \delta(k_0 + \omega_Q^l - \omega_\sigma^u) \right. \\ &\left. \frac{g^2 \text{Tr} [(\not{k} + m_Q)(\not{l} + m_Q)]}{m_Q (4\omega_Q^l \omega_\sigma^u)} \right]_{l_0=-\omega_Q^l, k_0=\omega_Q^k}, \quad (23) \end{aligned}$$

where $n_Q(\omega_Q^l)$ and $n_{\pi,\sigma}(\omega_{\pi,\sigma}^u)$ are the FD and BE distribution functions for intermediate Q and $M = \pi, \sigma$ states respectively. Analyzing the detailed branch cuts of this quark self-energy at finite temperature, one should notice that the quark pole ($k_0 = \omega_Q^k, \vec{k}$) remains within the Landau-cut region ($\vec{k} < k_0 < \{\vec{k}^2 + (m_Q - m_\pi)^2\}^{1/2}$) of $Q\pi$ loop, when $m_\pi > 2m_Q$. Therefore, we will get non-zero values of Γ_Q only in the temperature region, where $m_\pi > 2m_Q$. This Landau cut contribution of quark self-energy basically interprets forward and backward quark-meson scattering, by which mesons are absorbed and emitted respectively [20].

Similarly, thermal widths of pion and sigma mesons Γ_π and Γ_σ can be estimated from the retarded part of the meson self-energies $\Pi_{\pi(\pi\sigma)}^R$ and $\Pi_{\sigma(\pi\pi)}^R$ respectively, which are represented by Fig 1(b) in a general form. Using the interaction Lagrangian density (20), they are respectively derived as

$$\begin{aligned} \Gamma_\pi(\vec{k}) &= -\frac{1}{m_\pi} [\text{Im} \Pi_{\pi(\pi\sigma)}^R(k)]_{k_0=\omega_\pi^k} \\ &= \left[\int \frac{d^3 \vec{l}}{(2\pi)^3} \{ n_\pi(\omega_\pi^l) - n_\sigma(\omega_\sigma^u) \} \delta(k_0 + \omega_\pi^l - \omega_\sigma^u) \right. \\ &\left. \left(\frac{\lambda^2 f_\pi^2}{m_\pi} \right) \frac{1}{4\omega_\pi^l \omega_\sigma^u} \right]_{k_0=\omega_\pi^k} \quad (24) \end{aligned}$$

and

$$\begin{aligned} \Gamma_\sigma(\vec{k}) &= -\frac{1}{m_\sigma} [\text{Im} \Pi_{\sigma(\pi\pi)}^R(k)]_{k_0=\omega_\sigma^k} \\ &= \left[\int \frac{d^3 \vec{l}}{(2\pi)^3} \{ 1 + n_\pi(\omega_\pi^l) + n_\pi(\omega_\pi^u) \} \delta(k_0 - \omega_\pi^l - \omega_\pi^u) \right. \\ &\left. \left(\frac{\lambda^2 f_\pi^2}{m_\sigma} \right) \frac{1}{4\omega_\pi^l \omega_\pi^u} \right]_{k_0=\omega_\sigma^k}, \quad (25) \end{aligned}$$

where n_π and n_σ are BE distribution functions for intermediate π and σ states respectively.

Analyzing the detailed branch cuts of this pion and sigma meson self-energies at finite temperature, one can find that the pion pole ($k_0 = \omega_\pi^k, \vec{k}$) and sigma pole ($k_0 = \omega_\sigma^k, \vec{k}$) are respectively situated in the Landau-cut ($\vec{k} < k_0 < \{\vec{k}^2 + (m_\sigma - m_\pi)^2\}^{1/2}$) and unitary-cut ($\{\vec{k}^2 + (m_\pi + m_\sigma)^2\}^{1/2} < k_0 < \infty$) regions for certain temperature range, where $m_\sigma > 2m_\pi$. Here, Landau cut contribution of pion self-energy measures the probabilities of forward and backward $\pi\sigma$ scattering, where a σ

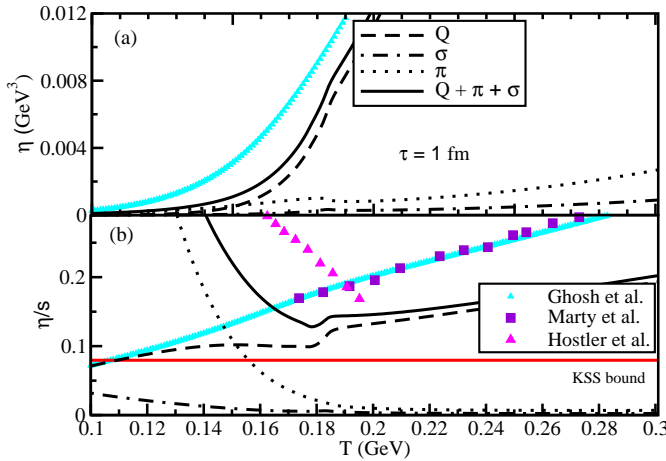


FIG. 2: (Color online) Temperature dependence of η (a) and η/s (b) for quark (dashed line), pion (dotted line), sigma (dash-dotted line) and their total (solid line) for constant relaxation time $\tau = 1$ fm. The results of Marty et al. [19] (blue squares), Ghosh et al. [20] (cyan triangles), Hostler et al. [16] (magenta triangles) are included for comparison. The straight horizontal red line indicates the KSS bound.

is absorbed by former process and emitted by latter one. Next, the unitary cut contribution of σ meson self-energy signifies forward and backward decay processes - $\sigma \rightarrow \pi\pi$ and $\pi\pi \rightarrow \sigma$ respectively. Unlike to the earlier Landau cuts for quark and pion self-energies, this unitary cuts of σ meson self-energy remains non-vanishing at $T = 0$ as it is associated with forward decay process. At finite temperature, this unitary cut contribution gives a Bose-enhanced probability of this forward decay process and also an in-medium probability of backward decay process, which was absent in vacuum.

III. RESULTS AND DISCUSSION

Let us start our numerical investigations by using the expressions of η , ζ and σ for constant values of thermal widths of medium constituents to highlight the effects arising from the phase space structure in the expressions of transport coefficients, Eqs. (11–16). The results of $\eta(T)$ for constant Γ_Q , Γ_π and Γ_σ are plotted by dashed, dotted and dash-dotted lines in Fig. 2(a). One can define their respective relaxation times τ_Q , τ_π and τ_σ using the relation $\tau_{(Q,\pi,\sigma)} = 1/\Gamma_{(Q,\pi,\sigma)}$ and we have fixed their values to 1 fm as a typical value. The total shear viscosity $\eta_t = \eta_Q + \eta_\pi + \eta_\sigma$ is denoted by solid line in Fig. 2(a), which exposes the dominant contribution of the quark component, compared to the contributions of the components π and σ mesons. $\eta(T)$ of all components and their total have appeared as increasing functions of T but they face some changes in their rate of increments near the transition temperature T_c .

The Fig. 2(b) shows the variation for η/s with temperature for respective components and their total, where

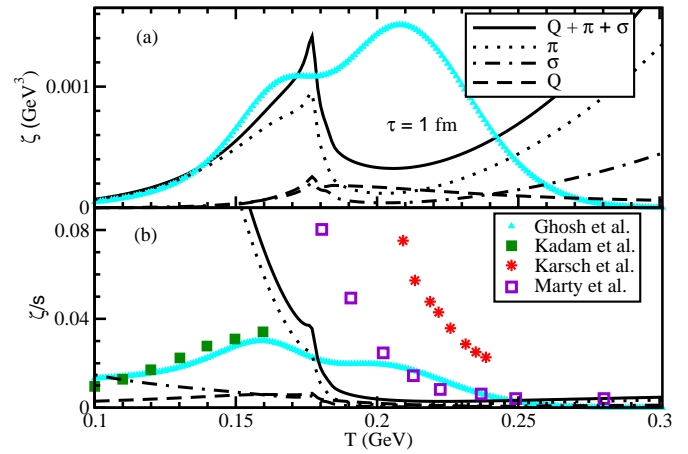


FIG. 3: (Color online) Temperature dependence of ζ (a) and ζ/s (b) of quark (dashed line), pion (dotted line), σ (dash-dotted line) and their total (solid line). The results are compared with Karsch et al. [43] (red stars), Kadam et al. [14] (solid green squares), Ghosh et al. [20] (cyan triangles) and Marty et al. [19] (open squares)

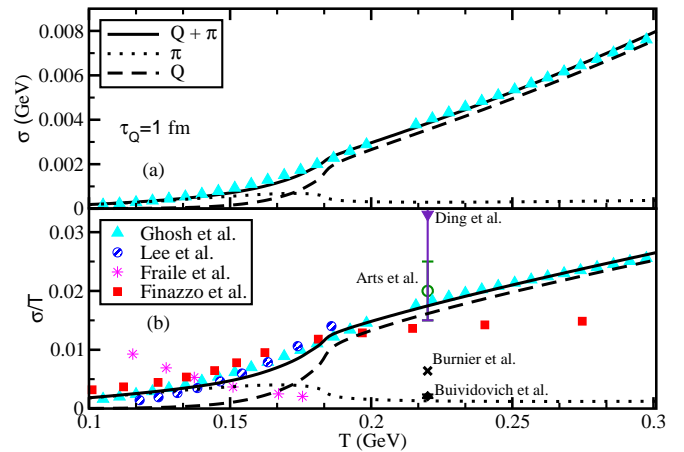


FIG. 4: (Color online) Temperature dependence of σ (a) and σ/T (b) for quark (dash line), pion (dotted line) components, and their total (solid line) in comparison with earlier results by Lee et al. [63] (solid blue circles), Ghosh et al. [20] (triangles up), Fraile et al. [9] (magenta stars), Finazzo et al. [62] (red squares), Ding et al. [51] (triangle down), Arts et al. [52] (open circle), Burnier et al. [54] (cross) and Buividovich et al. [53] (diamond).

we notice that mesonic components decrease and quark component increases with temperature. The increasing trend of total η/s at quark temperature domain is supported by the results of Ghosh et al. [20] (cyan triangles) and Marty et al. [19] (violet squares). The decreasing trend of the ratio below the transition temperature is also in agreement with the standard hadronic model calculations [7–16].

Following same notations of curves in Fig. (2), the temperature dependence of ζ and ζ/s are shown in Fig. 3(a)

and (b) respectively. Here, we are observing a sharp peak structure in ζ near T_c . To understand this, we have to focus on the conformal symmetry breaking terms [17, 20] $(\frac{1}{3} - c_s^2)$ and $\frac{d}{d\beta^2}(\beta^2 m_Q^2)$ in the integrand of Eq. (13). Near T_c , the contribution of these quantities become maximum, which is at the root of this peak structure in ζ . Hence, one can associate this peak structure of $\zeta(T)$ with the maximum violation of conformal symmetry breaking of quark matter near T_c . We get evidence of this fact from the earlier calculations, based on Linear Sigma Model [17, 39] and Nambu-Jona-Lasinio model [20], where similar kind of peak structure in ζ near T_c were observed. We may assume indication of similar kind of peak structure from the increasing nature of $\zeta/s(T < T_c)$ [14, 16] in the hadronic temperature range and the decreasing nature of $\zeta/s(T > T_c)$ [37, 42, 43] in the temperature region of quark phase. Fig. 3(b) has included some earlier results of ζ/s by Ghosh et al. [20] (triangles), Kadam et al. [14] (solid squares), Karsch et al. [43] (stars), Marty et al. [19] (open squares), whose order of magnitude is roughly close to the present estimations.

Next, Fig. 4(a) and (b) are respectively presenting the electrical conductivity σ and the dimensionless quantity σ/T for different components of the medium. Using Eqs. (15), (16) and (19), the results for quark (dashed line), pion (dotted line) components and their total (solid line) are generated, where charge neutral constituents like σ and π^0 will not come into the picture. Similar to shear viscosity, $\sigma(T)$ of different components and their total are appeared as increasing functions of T with some changes in their rate of increments near the transition temperature T_c . The $\sigma(T)$ of quark component is quite larger than that of pion component at high T domain but at low temperature domain, pion component is dominant over quark component. Our results of $\sigma(T)$ and $\sigma(T)/T$ are in quite well agreement with the results of Ghosh et al. [20] (cyan triangles). In the hadronic temperature domain, σ/T of Refs. [62–64] are more or less in same order of magnitude with us. In this context, there are large numbers of works in LQCD approach with different numerical strength of σ/T . Some of them [51–54] are displayed in Fig. 4(b) at certain T ($> T_c$).

So far, the results of transport coefficients η , ζ and σ are generated for constant Γ or τ of medium constituents. Now let us discuss the detail structure of thermal widths for different medium constituents and then the results of different transport coefficients using those temperature and momentum dependent Γ 's. For quark thermal width Γ_Q , let us first concentrate on Eq. (23), which gives the on-shell value ($k_0 = \omega_Q$) of the imaginary part of quark self-energy for quark-meson loops. We can see the invariant mass distribution of Γ_Q by transforming the on-shell relation $k_0 = \omega_Q = \{\vec{k}^2 + m_Q^2\}^{1/2}$ to the off-shell one $k_0 = \{\vec{k}^2 + M^2\}^{1/2}$ in Eq. (23), where M is invariant mass of quark. For a particular temperature $T = 0.120$ GeV and quark momentum $\vec{k} = 0.500$ GeV,

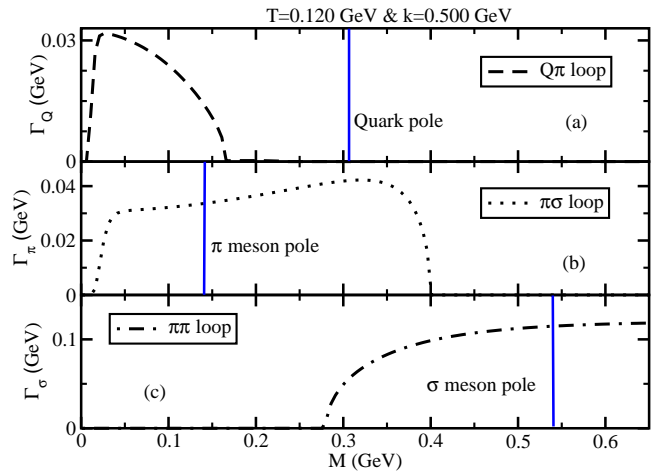


FIG. 5: (Color online) Invariant mass distribution of thermal width of quark (a), pion (b) and sigma meson (c) at $T = 0.120$ GeV and $|\vec{k}| = 0.500$ GeV. The vertical blue lines in each panel correspond to the pole mass of the respective particles.

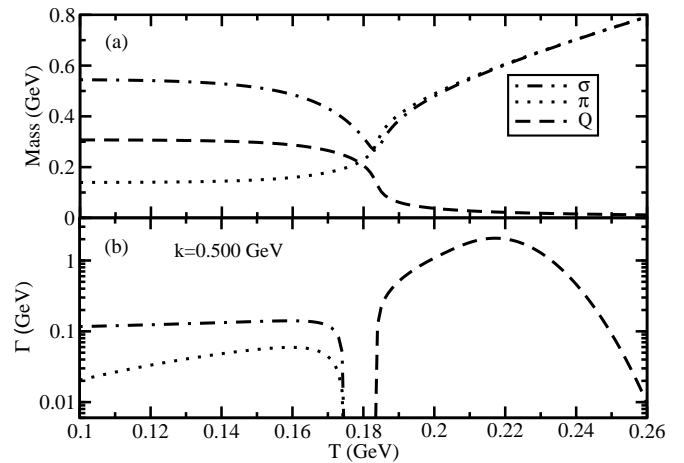


FIG. 6: Temperature dependence of mass (a) and thermal width (b) for quark (dash line), pion (dotted line) and sigma meson (dash-dotted line). Momentum is fixed at $|\vec{k}| = 0.500$ GeV for panel (b).

Fig. 5(a) shows the structure of $\Gamma_Q(M)$ (dash line). Here the straight vertical blue line denotes the on-shell (constituent) quark mass m_Q at $T = 0.120$ GeV, obtained within PQM model. We can see that the m_Q is away from the Landau cut region ($0 < M < |m_Q - m_\pi|$) of quark self-energy, where $\Gamma_Q(M)$ is non-zero. Therefore, on-shell value of Γ_Q at $T = 0.120$ GeV is zero, which we can see from the dash line of Fig. 6(b). Remembering the discussion related to this issue after Eq. (23), we can get non-zero on-shell value of Γ_Q beyond the Mott temperature T_M , from where the threshold condition ($m_\pi > 2m_Q$) of πQQ interaction will be valid. In other words, we can say that m_Q will be within the Landau cut region of quark self-energy for $T > T_M$.

Imposing similar kind of off-shell condition in Eqs. (24)

and (25) for π and σ mesons, one obtains $\Gamma_\pi(M)$ and $\Gamma_\sigma(M)$ which are shown in Fig. 5(b) and (c) respectively. We see that the on-shell masses of π and σ mesons at $T = 0.120$ GeV, indicated by blue vertical lines in Fig. 5(b) and (c), are located within the respective branch cuts of their self-energies. Therefore, we will get non-zero on-shell values of Γ_π and Γ_σ at $T = 0.120$ GeV. After a certain temperature, from where the threshold condition ($m_\sigma > 2m_\pi$) of $\sigma\pi\pi$ interaction is not valid, the on-shell values of Γ_π and Γ_σ will vanish. This fact becomes more clear in Fig. 6(b), where on-shell values of Γ_π (dotted line), Γ_σ (dash-dotted line) and Γ_Q (dashed line) are plotted against T axis. We notice that Γ_π and Γ_σ become non-zero at hadronic temperature range and beyond a certain temperature they vanish, whereas Γ_Q remains zero in hadronic temperature region and beyond a temperature, it gets the non-zero value. These interesting features are mainly controlled by the T dependence of m_Q , m_π and m_σ , as shown by dashed, dotted and dash-dotted lines respectively in Fig. 6(a). The masses of σ and π mesons are basically obtained from the Eqs. (6) and (8). In the chirally broken phase, the pion mass, being the mass of an approximate Goldstone mode is protected and varies weakly with temperature. On the other hand, the mass of σ , which is approximately twice the constituent quark mass, drops significantly near the transition temperature. At high temperature, being chiral partners, the masses of σ and π mesons become degenerate and increase linearly with temperature. The temperature dependence of quark mass $m_q = g \sigma$ is mainly tuned by temperature dependence of chiral order parameter σ , which decreases with temperature to small values but never vanishes. On the other hand, the Polyakov loop parameter grows from $\Phi(T = 0) = 0$ to $\Phi = 1$ at high temperatures. These decreasing and increasing nature of $\sigma(T)$ and $\Phi(T)$ respectively have important association with the chiral and confinement properties of quark-hadron phase transition. Thus we observe that these informations of the phase structure that enter into the temperature dependence of the masses of mesons and quark affect the calculations of the transport coefficients. The transport coefficients thus depend both on the phase space factors and the momentum dependent widths.

Using constant thermal widths, we have first explored how the temperature dependence of the phase space part make impact on transport coefficients. These are basically exposed in the earlier Figs. (2), (3) and (4).

Now replacing the constant $\Gamma_{(Q,\pi,\sigma)}$ by the explicit structure of $\Gamma_{(Q,\pi,\sigma)}$ in Eqs. (23), (24) and (25), the Figs. (2), (3) and (4) are respectively transformed to Figs. (7), (8) and (9), which have now additional influence of temperature dependent thermal widths along with the phase space part. We have split the temperature region into two parts because of the kinematic thresholds for mesons and quark self-energies. The first part, covering the hadronic temperature range, is for the results of pion component, while the results of quark component are plotted in the second part, which can be considered

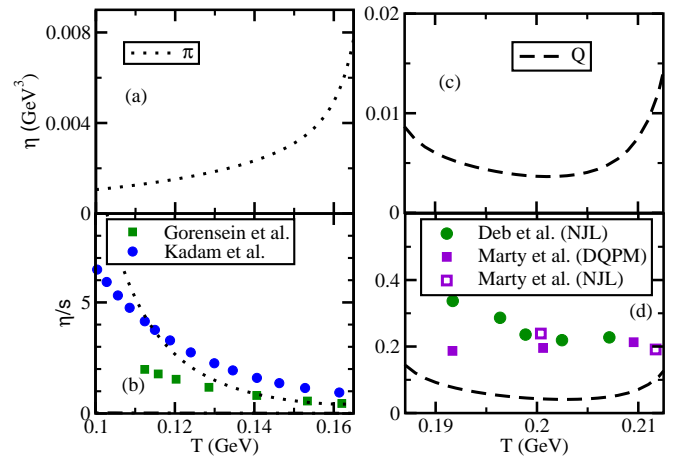


FIG. 7: (Color online) Temperature dependence of η (a) and η/s (b) for pion (dotted line) and quark (dashed line) using their temperature and momentum dependent thermal widths and comparison with the results of Kadam et al. [15] (blue circles), Gorenstein et al. [13] (green squares), Deb et al. [21] (green circles), Marty et al. [19] (solid and open squares for DQPM and NJL model).

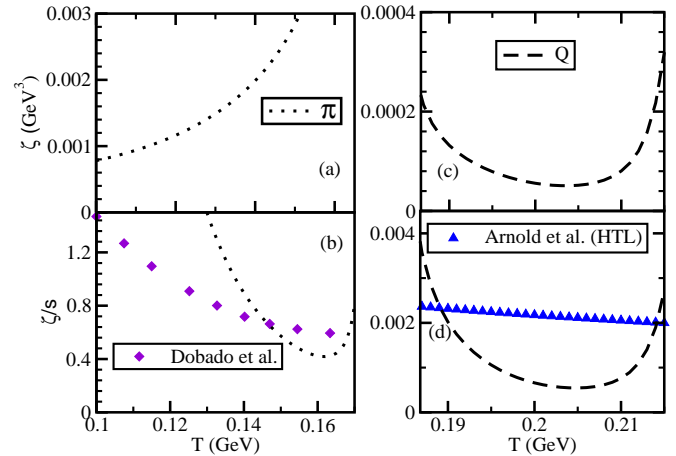


FIG. 8: (Color online) Temperature dependence of ζ (a) and ζ/s (b) of quark (dashed line) pion (dotted line) by using their temperature and momentum dependent thermal widths and compared with the results of Dobado et al. [39] (violet diamonds), Arnold et al. [35] (blue triangles).

as quark temperature region. Since the results of σ meson component is negligible, because of its high values of Γ_σ as well as m_σ in the hadronic temperature range, the results of pion component can only be visible in the panel of hadronic temperature region. Let us first come to the Fig. 7, where η and η/s for pion and quark components are described in panels (a), (b), (c) and (d) respectively. The blowing up tendency of η for pion component at high T domain is because of the suppressing tendency of Γ_π , as shown previously by the dotted line in Fig. 6(b). Similarly, the result of η for quark component is also limited within a particular (high) temperature domain because

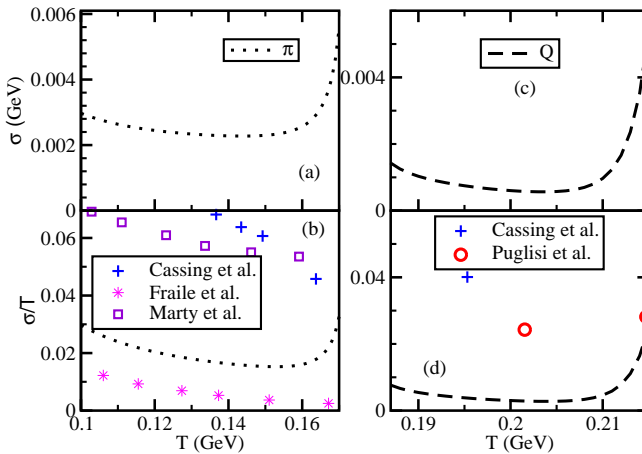


FIG. 9: (Color online) Temperature dependence of σ (a) and σ/T (b) for pion (dotted line) and quark (dashed line) using their temperature and momentum dependent thermal widths and comparison with the results of Fraile et al. [9] (magenta stars), Marty et al. [19] (open squares), Cassing et al. [58] (blue pluses), Puglisi et al. [59] (open circles).

the non-zero structure of $\Gamma_Q(T)$ is limited within that T -zone, as shown previously by dashed line in Fig. 6(b). That is why we should focus on the order of magnitude for the transport coefficients instead of those blowing up regions. Fig. 7(b) shows that the η/s for pion component from our calculation has approximately same order of magnitude with the results of Kadam et al. [15] (blue circles), Gorenstein et al. [13] (green squares). The corresponding results for quark component in its T range agree with the earlier results obtained by Deb et al. [21] (green circles) and Marty et al. [19] (solid and open squares for two different models). Following similar pattern of Fig. (7), Fig.8(a) to (d) are describing the ζ and ζ/s for pion and quark components, whose order of magnitude are comparable with results of Dobado et al. [39] (violet diamonds) in the hadronic temperature range and Arnold et al. [1, 35] (blue triangles) in the quark temperature domain. Next, using the same T and \vec{k} dependent thermal widths, the electrical conductivity σ and σ/T for pion and quark components are plotted in Fig. (9). Numerical values of σ/T , obtained by us, are compared with the results of Marty et al. [19] (open squares), Cass-

ing et al. [58] (blue pluses), Fraile et al. [9, 64] (magenta stars) in the hadronic temperature domain, whereas in the quark temperature domain, the values of our σ/T are compared with the results of Cassing et al. [58] (blue pluses) and Puglisi et al. [59] (open circles).

IV. SUMMARY

In this article, we have investigated the role of PQM dynamics in calculations of different transport coefficients like shear viscosity η , bulk viscosity ζ and electrical conductivity σ of quark and hadronic medium. We have started with the standard expressions of these transport coefficients, which are inversely proportional to the thermal width Γ of the medium constituents. Using those expressions for constant values of Γ , we have found the phase-space effect of PQM dynamics on their numerical values. The η and σ are appeared as increasing function of T with certain changes in increments at the quark-hadron phase transition point. In this regard, ζ has exhibited a peak structure near the transition temperature T_c . The nature of T dependence and absolute values of these transport coefficients more or less agree with some of the earlier works.

Then, we have considered an explicit temperature and momentum dependence of Γ for quark and mesons to estimate the values of those transport coefficients, where quark and meson thermal widths are calculated from the imaginary part of their self-energies at finite temperature. The thermal widths of quark and mesons are found to be non-zero at limited regions of high and low temperature domain because of their respective threshold conditions. Therefore, when we have estimated different transport coefficients by using those thermal widths, we are able to predict their values within those temperature ranges only, whose order of magnitude more or less agree with some of the earlier results.

Acknowledgment: SG is financially supported from University Grant Commission (UGC) Dr. D. S. Kothari Post Doctoral Fellowship (India) under grant No. F.4-2/2006 (BSR)/PH/15-16/0060. PS is supported from the scheme of DST Inspire (India). SG would like to thank to Sandeep Chatterjee, Bhaswar Chatterjee for initial motivative discussion on this work.

[1] J. I. Kapusta, *Relativistic Nuclear Collisions*, Landolt-Bornstein New Series, Vol. I/23, ed. R. Stock (Springer-Verlag, Berlin Heidelberg 2010).
[2] P. Romatschke and U. Romatschke, Phys. Rev. Lett. 99, 172301 (2007); T. Hirano and M. Gyulassy, Nucl. Phys. A769, 71 (2006).
[3] C. Gale, S. Jeon, and B. Schenke, Int. J. Mod. Phys. A28, 134011 (2013).
[4] P. B. Arnold, G. D. Moore, and L. G. Yaffe, J. High Energy Phys. 11 (2000) 001; 05 (2003) 051.
[5] N. Christiansen, M. Haas, J. M. Pawłowski, N. Strodthoff, Phys. Rev. Lett. 115, 112002 (2015).
[6] H. B. Meyer, Phys. Rev. D **76**, 101701 (2007); Phys. Rev. D **82**, 054504 (2010).
[7] K. Itakura, O. Morimatsu, and H. Otomo, Phys. Rev. D **77**, 014014 (2008).
[8] A. Dobado and S.N. Santalla, Phys. Rev. D **65**, 096011 (2002); A. Dobado and F. J. Llanes-Estrada, Phys. Rev. D **69**, 116004 (2004).
[9] D. Fernandez-Fraile and A. Gomez Nicola, Eur. Phys. J.

C **62**, 37 (2009).

[10] R. Lang, N. Kaiser and W. Weise Eur. Phys. J. **A** **48**, 109 (2012).

[11] S. Mitra, S. Ghosh, and S. Sarkar Phys. Rev. **C** **85**, 064917 (2012).

[12] S. Ghosh, G. Krein, S. Sarkar, Phys. Rev. **C** **89**, 045201 (2014); S. Ghosh, Phys. Rev. **C** **90** 025202 (2014); S. Ghosh, Braz. J. Phys. 45 (2015) 687.

[13] M. I. Gorenstein, M. Hauer, O. N. Moroz, Phys. Rev. **C** **77**, 024911 (2008).

[14] G. P. Kadam and H. Mishra, Nucl. Phys. **A** **934**, 133 (2015).

[15] G. P. Kadam and H. Mishra, Phys. Rev. **C** **92**, 035203 (2015).

[16] J. Noronha-Hostler, J. Noronha, C. Greiner, Phys. Rev. Lett. **103**, 172302 (2009).

[17] P. Chakraborty and J. I. Kapusta, Phys. Rev. **C** **83**, 014906 (2011).

[18] C. Sasaki, K. Redlich, Nucl. Phys. **A** **832** (2010) 62.

[19] R. Marty, E. Bratkovskaya, W. Cassing, J. Aichelin, H. Berrehrah, Phys. Rev. **C** **88** (2013) 045204.

[20] S. Ghosh, T. C. Peixoto, V. Roy, F. E. Serna, and G. Krein, Phys. Rev. **C** **93**, 045205 (2016).

[21] P. Deb, G. Kadam, H. Mishra, Phys. Rev. **D** **94** (2016), 094002.

[22] A. N. Tawfik, A. M. Diab, M.T. Hussein, Int.J.Mod.Phys. A31 (2016) 1650175; arXiv:1610.06041 [nucl-th].

[23] S. Ghosh, A. Lahiri, S. Majumder, R. Ray, S. K. Ghosh, Phys. Rev. **C** **88** (2013) 068201.

[24] R. Lang, W. Weise Eur. Phys. J. **A** **50**, 63 (2014); R. Lang, N. Kaiser, W. Weise, Eur. Phys. J. **A** **51**, 127 (2015).

[25] S. K. Ghosh, S. Raha, R. Ray, K. Saha, S. Upadhyaya, Phys. Rev. **D** **91**, 054005 (2015).

[26] N. Demir and S.A. Bass Phys. Rev. Lett. 102, 172302 (2009).

[27] A. Muronga, Phys. Rev. **C** **69**, 044901 (2004).

[28] S. Plumari, A. Puglisi, F. Scardina, and V. Greco, Phys. Rev. **C** **86**, 054902 (2012).

[29] S. Pal, Phys. Lett. **B** **684** (2010) 211.

[30] N. Sadooghi, F. Taghinevaz, Phys. Rev. **D** **89**, 125005 (2014).

[31] M. Albright and J. I. Kapusta, Phys. Rev. **C** **93**, 014903 (2016).

[32] M. Prakash, M. Prakash, R. Venugopalan, and G. Welke, Phys. Rep. 227, 321 (1993).

[33] S. Gavin, Nucl. Phys. **A**, **435**, 826 (1985).

[34] K. Paech and S. Pratt, Phys. Rev. **C** **74**, 014901 (2006).

[35] P. Arnold, C. Dogan, G. D. Moore, Phys. Rev. **D** **74**, 085021 (2006).

[36] S. K. Das, J. Alam Phys.Rev. **D** **83** (2011) 114011.

[37] H. B. Meyer, Phys. Rev. Lett. 100, (2008) 162001.

[38] A. Dobado, F.J.Llane-Estrada, J. Torres Rincon, Phys. Lett. **B** **702**, 43 (2011).

[39] A. Dobado, J. Torres Rincon, Phys. Rev. **D** **86**, 074021 (2012).

[40] C. Sasaki, K. Redlich, Phys. Rev. **C** **79**, 055207 (2009).

[41] X. Shi-Song, G. Pan-Pan, Z. Le, H. De-Fu, Chin. Phys. **C** **38**, (2014) 054101.

[42] D. Kharzeev, K. Tuchin, JHEP **0809**, 093 (2008).

[43] F. Karsch, D. Kharzeev, K. Tuchin, Phys. Lett. **B** **663** (2008) 217.

[44] V. Chandra, Phys. Rev. **D** **86** (2012) 114008; Phys. Rev. **D** **84** (2011) 094025.

[45] D. Fernandez-Fraile and A. Gomez Nicola, Phys. Rev. Lett. **102**, 121601 (2009).

[46] S. Mitra and S. Sarkar, Phys. Rev. **D** **87**, 094026 (2013); S. Mitra, S. Gangopadhyaya, and S. Sarkar, Phys. Rev. **D** **91**, 094012 (2015).

[47] S. Ghosh, S. Chatterjee, B. Mohanty Phys. Rev. **C** **94** (2016) 045208.

[48] G. Sarwar, S. Chatterjee, Jane Alam arXiv: 1512.06496[nucl-th].

[49] G. P. Kadam, H. Mishra, Phys.Rev. **C** **93** (2016) 025205.

[50] K. Saha, S. Upadhyaya, S. Ghosh, Mod. Phys. Lett. **A** **32** (2016) no.05, 1750018.

[51] H.T. Ding, A. Francis, O. Kaczmarek, F. Karsch, E. Laermann, and W. Soeldner, Phys. Rev. D 83, 034504 (2011).

[52] G. Aarts, C. Allton, J. Foley, S. Hands, and S. Kim, Phys. Rev. Lett. 99, 022002 (2007).

[53] P. V. Buiividovich, M. N. Chernodub, D. E. Kharzeev, T. Kalaydzhyan, E. V. Luschevskaya, and M. I. Polikarpov, Phys. Rev. Lett. 105, 132001 (2010).

[54] Y. Burnier and M. Laine, Eur. Phys. J. C 72, 1902 (2012).

[55] S. Gupta, Phys. Lett. B 597, 57 (2004).

[56] B. B. Brandt, A. Francis, H. B. Meyer, and H. Wittig, J. High Energy Phys. 03 (2013) 100.

[57] A. Amato, G. Aarts, C. Allton, P. Giudice, S. Hands, J.I. Skullerud, Phys. Rev. Lett. 111, 172001 (2013).

[58] W. Cassing, O. Linnyk, T. Steinert, and V. Ozvenchuk, Phys. Rev. Lett. 110, 182301 (2013).

[59] A. Puglisi, S. Plumari, V. Greco, Phys. Rev. **D** **90**, 114009 (2014); J. Phys. Conf. Ser. 612 (2015) 012057; Phys. Lett. **B** **751** (2015) 326.

[60] M. Greif, I. Bouras, Z. Xu, C. Greiner, Phys. Rev. **D** **90** (2014) 094014; J. Phys. Conf. Ser. 612 (2015) 012056.

[61] P. K. Srivastava, L. Thakur, B. K. Patra, Phys. Rev. **C** **91**, 044903 (2015).

[62] S. I. Finazzo, J. Noronha Phys. Rev. D 89, 106008 (2014).

[63] C. Lee, I. Zahed, Phys. Rev. C 90, 025204 (2014).

[64] D. Fernandez-Fraile and A. Gomez Nicola, Phys. Rev. D 73, 045025 (2006).

[65] M. Greif, C. Greiner, G.S. Denicol, Phys. Rev. D 93, 096012 (2016).

[66] S. Ghosh, F. E. Serna, G. Krein, *in progress*

[67] S. Mitra and V. Chandra, Phys. Rev. **D** **94**, 034025 (2016).

[68] S. Ghosh, Phys. Rev. **D** **95** (2017) 036018.

[69] B.-J. Schaefer, J. M. Pawłowski, J. Wambach, Phys. Rev. **D** **76**, 074023 (2007).

[70] S. Ghosh, Int. J. Mod. Phys. **A** **29** (2014) 1450054.

[71] P. Kovtun, D. T. Son, and O. A. Starinets, Phys. Rev. Lett. 94, 111601 (2005).